Interface stability in hybrid metal-oxide magnetic trilayer junctions

J. Z. Sun
IBM T. J. Watson Research Center, P.O. Box 218, Yorktown Heights, New York 10598

K. P. Roche and S. S. P. Parkin
IBM Almaden Research Center, 650 Harry Road, San Jose, California 95120

(Received 12 October 1999; revised manuscript received 4 January 2000)

We show that for hybrid oxide-metal trilayer junctions of $Co_{0.8}Fe_{0.2}$-$SrTiO_3$-$La_{0.67}Sr_{0.33}MnO_3$ and Fe-$SrTiO_3$-$La_{0.67}Sr_{0.33}MnO_3$, the sign and field dependence of junction magnetoresistance are sensitive to the junction interface condition. Both positive and negative magnetoresistance can be obtained in either system, depending on the state of the junction interface. For high biases above 0.5 V, junction resistance shows time-dependent creep. The magnitude and direction of the creep depend on the magnitude and direction of the applied bias, indicating reversible structural modification of the junction interface. For these junctions, the interface chemistry, rather than fundamental band structures of the electrode materials, appears responsible for the observed sign-change of junction magnetoresistance.

In spin-polarized tunneling junctions, a sign change of junction magnetoresistance (MR) is occasionally observed. For some junctions the sign of MR is shown to depend on the bias voltage across the device, or on the choice of different combination of barrier and electrodes.[1–4] For example, cobalt electrode with $SrTiO_3$ or $Ce_{0.69}La_{0.31}O_{1.845}$ barrier and $La_{0.7}Sr_{0.3}MnO_3$ base is shown to have positive MR at certain bias, and negative MR at other bias, while the same structure with AlO_x barrier appears to have negative MR regardless of bias.[1,2] Other junctions showing a bias-dependent sign reversal include Permalloy electrode on top of a Ta_2O_5-AlO_x barrier,[3] and junctions of the type $Fe_3O_4/SrTiO_3/La_{0.7}Sr_{0.3}MnO_3$.[4] It is suggested[1,2] that the phenomenon is caused by a change in the alignment of the majority and minority electronic density of states between the two electrodes at the junction interface.

Here we investigate this phenomenon in model systems of $Co_{0.8}Fe_{0.2}$-$SrTiO_3$-$La_{0.67}Sr_{0.33}MnO_3$ (CoFe-STO-LSMO) and Fe-$SrTiO_3$-$La_{0.67}Sr_{0.33}MnO_3$ (Fe-STO-LSMO). Our results show that for junctions with $SrTiO_3$ barriers, there is another important factor contributing to the MR behavior of the junction. The additional factor is the oxygen mobility-related interface chemistry between the transition metal and $SrTiO_3$.

Junctions for the study were fabricated from films deposited on $NdGaO_3(110)$ substrates. First an epitaxial layer of $La_{0.67}Sr_{0.33}MnO_3$, about 600 Å thick, was deposited using laser ablation at a nominal substrate temperature of 750 °C in 300 mTorr of oxygen. A thin layer of $SrTiO_3$, about 30 Å thick, is epitaxially deposited immediately after, under the same condition. The film was cooled to ambient in 1 atm of oxygen, and transferred to another vacuum system for deposition of counter electrode. A plasma oxygen cleaning was done immediately prior to counter-electrode deposition. Counter electrodes of Fe or $Co_{0.80}Fe_{0.20}$, 100 Å thick, were then sputter deposited. The film was capped by 100 Å of titanium, and removed from vacuum for processing.

Optical photolithography was used to pattern the junction structure. The minimum junction feature was 1×1 μm^2, formed for the top ferromagnetic electrode. Electrical contact to the top electrode was made through a self-aligned lift-off window in an SiO_2 insulator layer that separates the top and bottom electrodes. The SiO_2 was about 1000 Å thick. This fabrication process has been discussed elsewhere.[5] The highest temperature the samples were exposed to during processing was 90 °C for an accumulated duration of less than 10 min. Junctions thus processed were wire-bonded to a sample holder and mounted to a close-cycle refrigerator-cooled cold finger for measurements.

Junction MR was measured in a magnetic field applied parallel to the film surface. Field alignments are illustrated in data plots shown below. The magnetic field was continuously swept during measurements at a frequency of 0.077 Hz. In all measurements, the positive terminal denotes the base LSMO electrode. Thus a positive bias has current flowing from LSMO through the barrier to the top ferromagnetic metal electrode. Electrons flow in opposite direction. The bottom electrode, LSMO, is a 33% hole-doped *p*-type metal. The transition-metal counter electrodes are *n* type. The barrier is $SrTiO_3$ which when fully oxygenated is a semiconductor with a calculated band gap around 5.1 eV.[6]

Junction resistance shows a complex temperature dependence. Figure 1 is a typical resistance vs temperature $R(T)$, plot for each of the two types of junctions. For temperatures below 50 K, junction resistance increases upon cooling. This is consistent in direction with a simple metal-insulator-metal tunneling picture,[7] although the magnitude of resistance change appears large. This may suggest additional suppression of the effective tunneling density of state at low temperature, which is a common feature seen in trilayer junctions involving manganite electrodes,[5] though not well understood. The decrease of $R(T)$ for temperatures above 250 K is probably related to thermal population of impurity sites within the $SrTiO_3$ barrier. The rise of junction resistance in the temperature range of 50 to 200 K is not well understood. These $R(T)$ data were shown as a part of general junction characterization. In this study, we focus only on the

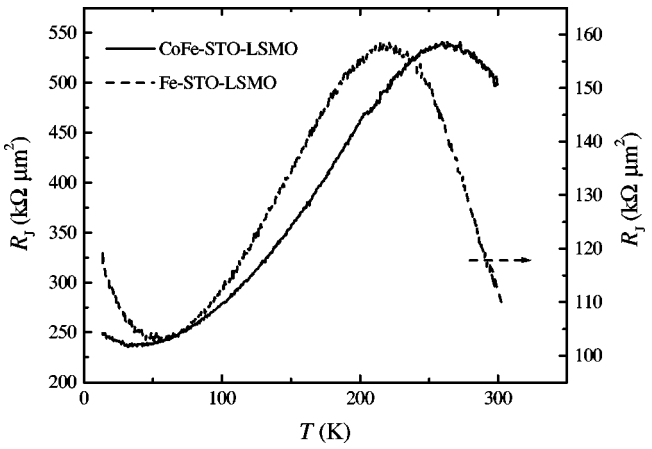

FIG. 1. The temperature dependence of junction resistance.

behavior of low-temperature junction magnetoresistance at 13 K as a function of magnetic field and bias current.

The base electrode $R_\square$ at 13 K was measured to be between 30 and 60 Ω. It assures that junction resistance stay well above $10\times R_\square$, which is necessary for preventing current distribution-induced false measurement of junction resistance[8] and especially junction MR.[9] This condition is not satisfied for junctions presented in Ref. 1. It could contribute to an enhanced reading of junction MR.

For this study we define the sign of magnetoresistance to be the same as $[R(H)-R(0)]/R(H)$, where $R(H)$ is the resistance value at ±3.5 kOe, and $R(0)$ is that in the low-field region. The magnitude of MR is determined from the minimum and maximum resistance value in the $R(H)$ sweep within ±3.5 kOe. All $R(H)$ curves shown are 10-trace averaged results. For an Fe-STO-LSMO junction, a negative

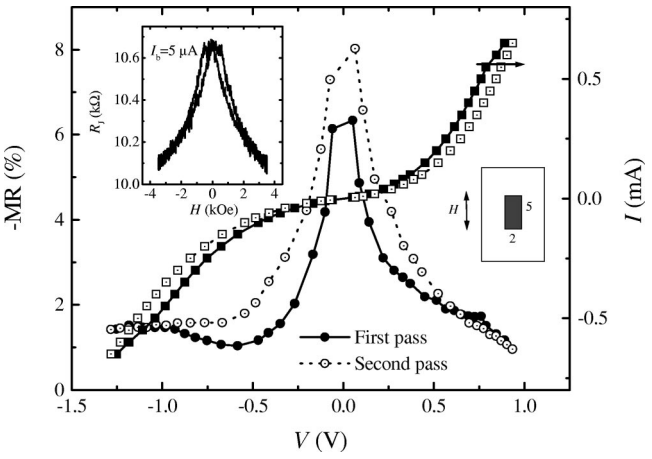

FIG. 2. An Fe-STO-LSMO junction with negative MR. Left axis: MR as a function of bias voltage. Right axis: I-V characteristics of the junction. Solid symbols represent first sweep of bias current. Open symbols, second sweep. To observe the consequence of high current stress on junction properties, bias sweeps were done with increasing *amplitude* of bias current, alternating between forward and backward biasing. A slight increase in junction resistance and MR is seen after the junction has experienced a high bias current, as evidenced by the difference in I-V and MR curve. Upper inset: the $R(H)$ curve during the first pass. Lower inset: junction geometry and the direction of applied field, numbers represent dimensions in μm.

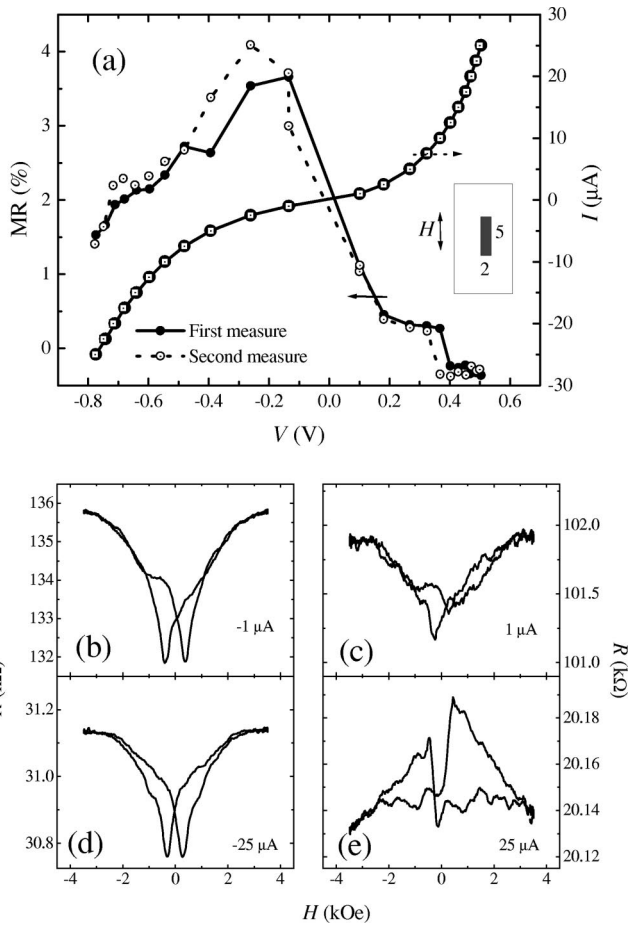

FIG. 3. Another Fe-STO-LSMO junction on the same chip, only 200 μm away from the one discussed before, showing positive MR at low bias. This junction is about ten times more resistive than the one discussed in Fig. 2. Upper panel shows MR and I-V characteristics. Lower panels show representative shapes of $R(H)$ at bias currents of ±1 and ±25 μA, respectively.

MR is observed at all bias voltages up to 1 V, as illustrated in Fig. 2. For another junction on the same chip, just 200 μm away, a positive MR is observed with a strong asymmetric bias-dependence, as shown in Fig. 3. For a CoFe-STO-LSMO junction, a negative MR is initially observed in both bias directions at low voltage. Upon biasing up to close to 1 V, junction resistance irreversibly increased by a factor of 20. From then on, the MR changed sign for negative biases. This is shown in Fig. 4.

These observations show that junction MR depends sensitively on junction preparation and measurement history, which relates to junction interface condition. Choice of electrode material alone is insufficient to determine even its sign—Data in Figs. 2–4 show that both Fe- and FeCo-based junctions can have MR's of either positive or negative signs, depending on the specific junction condition and measurement history.

Importantly, spin-dependent tunneling is only sensitive to the magnetic state several monolayers into the electrode from the tunneling interface.[10,11] Any interface transition region, such as an interface oxide layer between the transition metal and the $SrTiO_3$ barrier, will significantly affect the spin-transport characteristics of the junction. Also, in such a situation the magnetic moment at the junction interface may

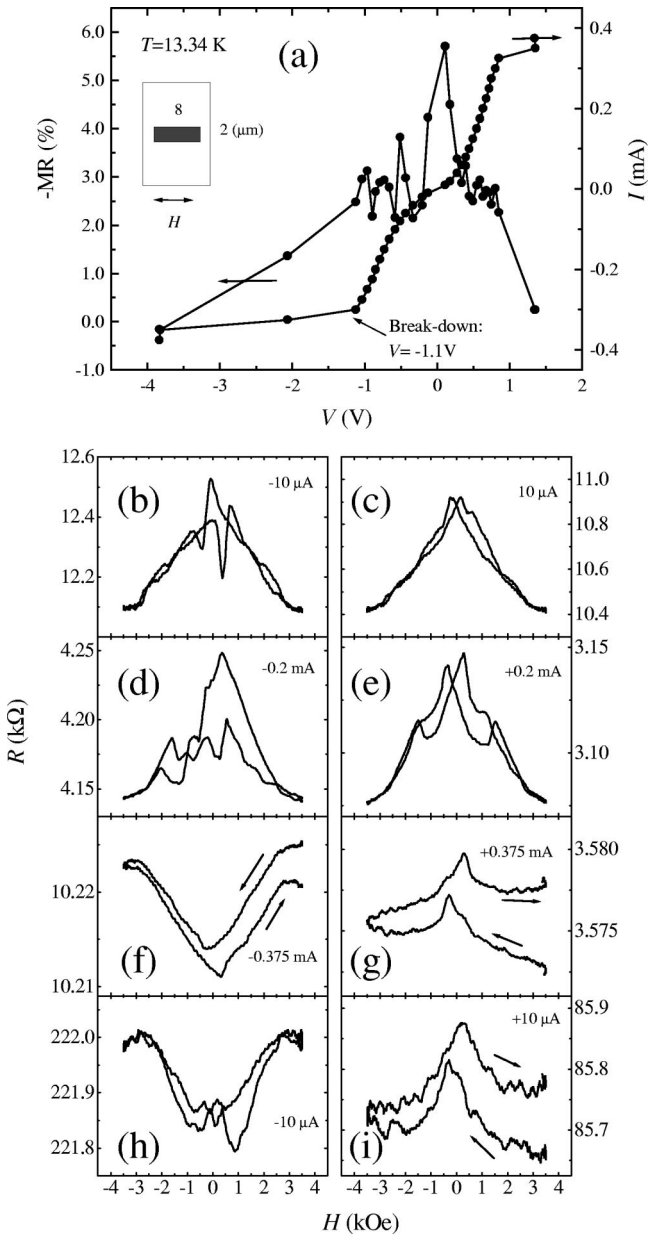

FIG. 4. A CoFe-STO-LSMO junction showing a bias-induced reversal of the sign of MR. (a) MR *vs* bias voltage and I-V characteristics. Inset: junction geometry and field direction. (b)–(g) show the $R(H)$ behavior at successively higher bias current. At a bias current of $-375\ \mu$A (f), junction MR reversed its sign, the low-bias junction resistance increased by a factor of 20. This change of junction characteristics is irreversible, as shown by subsequent measurements at a reduced bias current of $\pm 10\ \mu$A in (h) and (i). The drift in (f)–(i) is related to junction resistance-creep that is discussed below.

assume a very different orientation than those of the electrodes on average.

Experimentally, the general shape of $R(H)$ observed in our junctions show a significant high-field slope, indicating the presence of unsaturated magnetic moments at the junction interface. This points to a junction interface with different magnetic characteristics from that of the native electrode.

The shape of $R(H)$ is complex, especially for junctions with strong I-V asymmetry and reversal of MR's, such as the ones shown in Fig. 4. This could indicate a complex domain

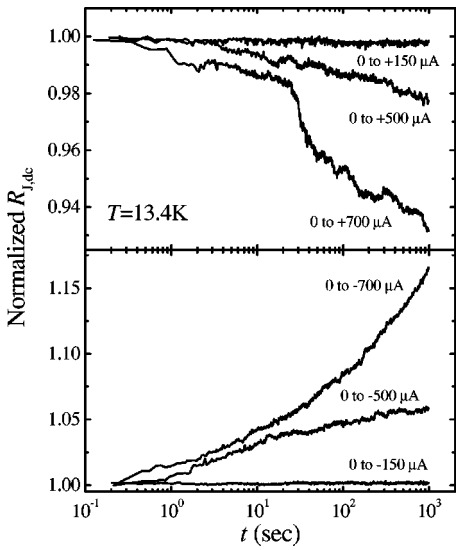

FIG. 5. At high bias currents, junction resistance show significant creep. The direction of resistance creep depends on polarity of the bias current, the rate of creep increases with increasing magnitude of the bias current.

switching process, as well as the presence of inhomogeneous current paths across the junction barrier. This is because the shape of $R(H)$ is determined by the average behavior of relative alignment of magnetic moments of the top and bottom electrodes at the points of junction interface that contribute to the spin-dependent transport.

Inhomogeneous transport and barrier inhomogeneity are also implicated by the observation of a *bias dependence* for shape of $R(H)$ as shown in Figs. 3 and 4. This can be understood in light of multiple current paths that sample different local magnetic states. The weight of each path to the overall $R(H)$ shape could vary as a function of bias, thus causing different shapes of $R(H)$ at different bias.

Barrier inhomogeneity certainly exists over a macroscopic length scale of several microns. Junction resistances were seen to scatter over two orders of magnitude, both for room temperature resistance and for low-temperature (13.4 K) resistance.

A natural consequence of inhomogeneous junction conduction is locally concentrated current flow. The average current density for measurements presented in Figs. 2–4 is on the order of 10^3 A/cm^2, the local current density involved could be much higher.

For junctions under high bias, a resistance creep was observed. Prior to irreversible change at the damage threshold, junction resistance creeps reversibly to higher or lower value, depending on the direction of the bias current. This phenomenon is summarized in Fig. 5. The junction studied here is $6\times 2\ \mu$m in size. Thus the areal-averaged current density applied, at 700 μA, is around 5.8×10^3 A/cm^2. The creep increases resistance when electrons are flowing from STO to the top metal electrode, and it decreases junction resistance when electrons are flowing into STO from the top electrode. The creep rate increases as bias current is increased in magnitude. Application of a static magnetic field up to 3 kOe does not affect the resistance creep rate. This is qualitatively similar to what was observed in superconducting tunneling junctions with an indium-oxide barrier.[12,13]

One possible cause for junction resistance creep here is oxygen electromigration. It is known that oxygen atoms are quite mobile in perovskite-type compounds. In the cuperate which is a close cousin of $SrTiO_3$ and LSMO, electromigration has been observed systematically.[14] Oxygen migration was also viewed as a leading cause of junction resistance creep in the case of superconducting junctions with InO_x barriers.[13] In our case, electromigration might cause a reversible oxidation of the top ferromagnetic metal electrode, creating an interface layer with altered magnetic properties between the electrode and the $SrTiO_3$ barrier. It is likely that the magnetic properties of this intermediate layer would determine the behavior of a junction's MR.

In summary, our observations suggest the presence of an unstable junction interface between $SrTiO_3$ and transition-metal electrodes such as Co and CoFe. A variation of this interface will profoundly change a junction's MR characteristics. This factor should be taken into account when one attempts to obtain a quantitative understanding of the magnetoresistance in magnetic tunneling junctions.

The authors wish to thank Bill Gallagher's group for help during sample preparation.

[1] J.M. De Teresa, A. Barthelemy, A. Fert, J.P. Contour, R. Lyonnet, F. Montaigne, P. Seneor, and A. Vaurès, Phys. Rev. Lett. **82**, 4288 (1999).

[2] Jose Maria De Teresa, Agnès Barthélémy, Albert Fert, Jean Pierre Contour, François Montaigne, and Pierre Seneor, Science **286**, 507 (1999).

[3] M. Sharma, S.X. Wang, and J.H. Nickel, Phys. Rev. Lett. **82**, 616 (1999).

[4] K. Ghosh, S.B. Ogale, S.P. Pai, M. Robson, Eric Li, I. Jin, Zi-wen Dong, R.L. Greene, R. Ramesh, T. Venkatesan, and M. Johnson, Appl. Phys. Lett. **73**, 689 (1998).

[5] J.Z. Sun, D.W. Abraham, K. Roche, and S.S.P. Parkin, Appl. Phys. Lett. **73**, 1008 (1998).

[6] L.F. Mattheiss, Phys. Rev. B **6**, 4718 (1972); **6**, 4740 (1972).

[7] E. L. Wolf, *Principles of Electron Tunneling Spectroscopy* (Oxford University Press, Oxford, 1985).

[8] R.J. Pedersen and F.L. Vernon, Appl. Phys. Lett. **10**, 29 (1967).

[9] R.J.M. Van de Veerdonk, J. Nowak, R. Meservey, J.S. Moodera, and W.J.M. De Jonge, Appl. Phys. Lett. **71**, 2839 (1997).

[10] Jagadeesh S. Moodera, Janusz Nowak, and Rene J. M. van de Veerdonk, Phys. Rev. Lett. **80**, 2941 (1998).

[11] Jagadeesh S. Moodera *et al.*, Phys. Rev. Lett. **83**, 3029 (1999).

[12] K.H. Gundlach and H. Konishi, Appl. Phys. Lett. **46**, 441 (1985).

[13] H. Kohlstedt, K.-H. Gundlach, and S. Kuriki, J. Appl. Phys. **73**, 2564 (1993).

[14] B.H. Moeckly, D.K. Lathrop, and R.A. Buhrman, Phys. Rev. B **47**, 400 (1993).